Determination of Thermophysical Properties and Boundary Conditions of Direct Chill–Cast Aluminum Alloys Using Inverse Methods

J.-M. DREZET, M. RAPPAZ, G.-U. GRÜN, and M. GREMAUD

In order to quantify the cooling conditions undergone by an ingot during direct-chill (DC) casting, thermocouples were immersed in the liquid pool and consequently entrapped in the solid, thus monitoring the temperature of the metal during its descent. Assuming steady-state thermal conditions, the time-dependent temperatures measured by these thermocouples were then converted into space-dependent temperature profiles. These values were the input of a *Maximum A Posteriori* (MAP) inverse method described by Rappaz *et al.*,[1] which has been adapted in this case to steady-state thermal conditions. This MAP method permits the deduction of the temperature-dependent thermal conductivity of the alloy, initially, and then of the highly nonuniform heat-flux distribution along the ingot rolling faces, in a second step. The obtained values are in good agreement with literature and clearly reflect the widely different boundary conditions associated with primary cooling (contact with the mold) and secondary cooling (water jet).

I. INTRODUCTION

IN the direct-chill (DC) casting of nearly rectangular rolling-sheet ingots and extrusion billets of aluminum alloys, a stationary temperature distribution gradually develops in the solidifying strand.[2] During cooling, the metal experiences a high nouniform thermal gradient, which results in differential thermal contraction and high stress levels partially relieved by creep. In this process, two distinct zones of cooling can be distinguished: the first one is due to the direct contact of the melt with the mold and the second one is associated with the water spray underneath. This leads to the formation of a thin solid shell that remains nearly parallel to the mold in between the two cooling zones. This thin shell bends inward under the high local thermal gradient, while the influence of the metallostatic pressure can be neglected.[3] An accurate description of the heat-transfer characteristics at the surface of the ingot in run conditions is important in many respects, for example, for a better understanding of the development of surface segregation and exudation.[4] It is also an essential input for thermomechanical models aimed at computing ingot distortions and stresses.[5]

The DC casting of aluminum alloys has been the subject of considerable development in recent decades, mostly as a result of an improved understanding of the heat flow involved. Yu[6] studied the heat-transfer mechanisms by quenching preheated probes in water. He showed that, in the case of DC casting, the ingot cooling rate highly depends on boiling water phenomena. Four mechanisms were distinguished by Incropera and de Witt,[7] depending on the target surface temperature: unstable film boiling, film boiling, nucleate boiling, and convection. Weckman and Niessen[8] built a numerical model based on the finite-element method to compute the steady-state temperature field in DC-cast AA6063 billets. Using a combination of theories involving nucleate boiling, forced convection, and film cooling, these authors developed a method to calculate the external boundary conditions associated with the casting configuration. Nevertheless, the authors showed that direct application of the theoretical coefficients would produce substantial errors, especially in the region where heat transfer is dominated by nucleate boiling. Grandfield *et al.*[9,10] discussed the heat-transfer mechanisms in the water jet and falling water film, with special attention paid to the boiling modes. They pointed out that, under normal steady-state conditions, nucleate boiling is the dominant phenomenon, but some areas of unstable film boiling can exist near the impingement point of the water jet. In the transient situation of the cast start, film boiling is also possible.

With the development of numerical models of the DC casting process, obtaining reliable heat-transfer data became essential. Based on *in-situ* temperature measurements in DC-cast ingots, Bakken and Bergström[11] and Jensen *et al.*[12] developed a method for the determination of the heat extracted by the cooling water and the mold. A third-order collocation polynomial was fitted to temperatures measured in the ingot in order to deduce the unknown temperature at the surface. More recently, Maenner *et al.*[13] and Opstelten and Rabenberg[14] studied the cooling of an instrumented solid aluminum block. After uniform heating, the block was cooled by an ascending water film, which simulated the steady-state situation of the secondary cooling in the actual DC casting process. These authors could distinguish two different cooling zonses: the impingement zone of the water jet, characterized by a fairly high heat flux, and the zone located below, the so-called "streaming zone," where the heat flux was much lower. They also made clear that the classical description of a heat-transfer coefficient (or heat flux) as a function of the surface temperature alone does

J.-M. DREZET, Senior Scientist, and M. RAPPAZ, Professor, are with the Laboratoire de Métallurgie Physique, Ecole Polytechnique Fédérale de Lausanne, CH-1015 Lausanne, Switzerland. G.-U. GRÜN is with the Research and Development Centre, VAW Aluminum AG, D-53014 Bonn, Germany. M. GREMAUD is with Calcom SA, CH-1015 Lausanne, Switzerland.

Manuscript submitted August 18, 1999.

not accurately describe the thermal-boundary condition typical for the secondary cooling zone.

Accurate thermophysical properties are probably as important as boundary conditions for the simulation of the DC casting process. As a matter of fact, both can be determined from temperature measurements performed under well-defined conditions using *inverse methods.*[15,16] The basic idea of these methods is to replace the analytical function appearing in standard least-squares methods by the numerical solution obtained from a *direct* finite-element method (FEM) or finite-difference method (FDM) calculation. For time-dependent boundary conditions, the problem is ill-posed and can lead to instabilities if the time-steps are too small. Several regularization methods have been devised to alleviate this difficulty.[15] For the determination of thermophysical parameters (*e.g.*, thermal conductivity and/or specific heat), Milano and Scarpa[17] have modified the least-squares technique to include a *Maximum A Posteriori* (MAP) algorithm. Rappaz *et al.*[1] have shown how the MAP algorithm can be easily implemented into a direct FEM heat-flow code[18] in the case of transient situations. They presented several examples illustrating the potential of the technique for the determination of time- or space-dependent heat-transfer coefficients and temperature-dependent thermal conductivity.

In the present contribution, the MAP algorithm is adapted to the case of permanent situations, with particular emphasis on the steady-state regime of the DC casting process. This numerical method and its implementation in a commercial code are briefly presented in Section III, whereas Section II first describes the technique used to measure *in situ* the temperature field and the contraction of DC-cast ingots. Finally, the last two sections give two applications of this inverse method, based on the same experimental data set measured for an AA5182 alloy: the determination of the temperature-dependent thermal conductivity of the alloy (Section IV) and the estimation of the heat-flux distribution along the ingot surface (Section V).

II. EXPERIMENTAL

Experimental DC casting trials were carried out in the context of the EMPACT project, in which European partners (both from industry and university) have joined to develop simulation tools for the improvement of the DC casting process. This project focused on micro-macrosegregation, fluid flow, and thermomechanical phenomena. As part of this project, the determination of thermophysical properties of several commercial alloys and the estimation of boundary conditions were two important tasks. For that purpose, instrumented DC casting experiments were performed in various cast houses of the industrial partners.

The present contribution illustrates the application of the inverse method to one of the DC cast ingots, whose standard cross section was 1860 × 510 mm. The main parameters of the casting were a cast length of typically 3 to 4 m; a casting speed of 1 mm s^{-1} (60 mm min^{-1}); a water flow rate of 2.63 L per minute, applied on each centimeter of the perimeter of the cross section; and a distribution bag measuring 300 × 100 × 100 mm. The water chamber mold section is 75 mm in width and 117 mm in height, with a wall thickness of 12 mm. The results of the AA5182 aluminum alloy inoculated with a titanium boron master alloy are presented in this contribution (note its composition in Table I). Six casting trials were conducted with this alloys, and the L-rod measurements progressively improved. After presenting the L-rod technique, the measurements obtained at the sixth trial are shown.

Table I. Composition in Weight Percent of the AA5182 Alloy

Si	Fe	Mg	Mn	Cu	Cr	Ti	Zn	Al
0.068	0.121	3.999	0.252	0.023	0.0038	0.0018	0.015	balance

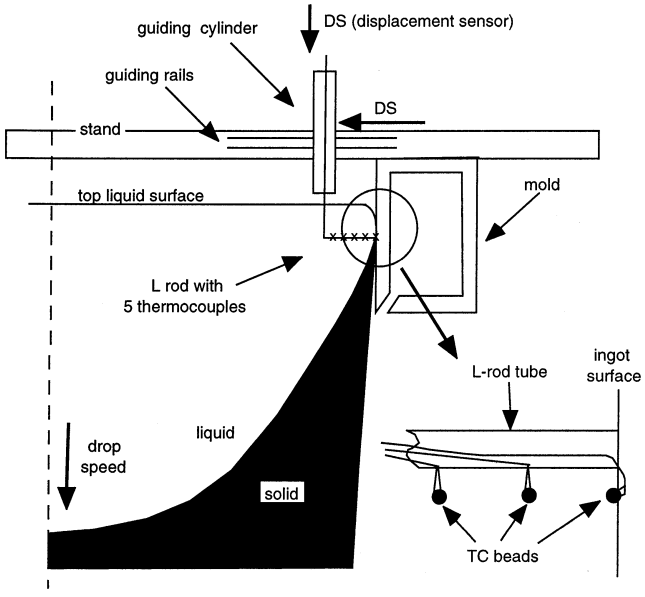

Fig. 1—Experimental setup used for the measurement of the temperature field along the ingot surface and of the metal surface displacement during DC casting. An enlargement of the extremity of the L-rod with the last three thermocouples is shown at the bottom right.

A. *The L-Rod Technique*

As shown schematically in Figure 1, the technique of the L-rod, first used by Drezet *et al.*,[3] is employed in the present study for the measurement of both temperatures and displacements. However, the quartz tube is replaced by a stainless steel one, which is more robust and better suited for use in cast houses. Five K-type thermocouples (chromel-alumel, with a single leg 0.2 mm in diameter) are placed within the 5-mm i.d. of the tube (6-mm o.d.), one of them being at the very surface of the ingot. The five beads, approximately 0.8 mm in diameter, are located 3 mm below the L-rod tube. Their final position is checked after solidification by X-ray inspection. It is to be noted that, as shown in Figure 1, the legs of the thermocouple located at the extremity of the L-rod emerge from the tube and bend inward, so that the junction can solidify with the ingot underneath at the very surface. Although the thermocouples are not calibrated, their precision is comparable to that of Reference 21, *i.e.*, about 1 °C, while their time response is on the order of 30 ms. The thermocouples are connected to a data-logger, and the temperatures are recorded every 0.25 seconds.

The whole setup is mounted on the wide side of the mold

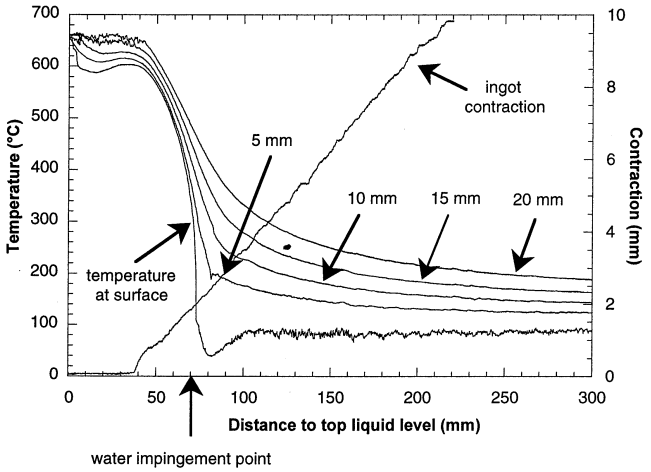

Fig. 2—Cooling curves recorded by the five thermocouples and ingot contraction inside the mold measured by the horizontal displacement of the L-rod.

(*i.e.*, along one of the rolling faces of the ingot), about 0.55 m from the short side. The design of the experiment allows the L-rod to move freely downward through a guiding cylinder. This cylinder is also free to move horizontally on two additional guiding rails. During the trials, the L-rod first drops into the liquid metal under its own weight before being "swallowed" by the mushy zone. From that instant, the L-rod moves downward at the casting speed of the ingot. When the solidifying metal shell pulls away from the mold surface, the lateral and vertical displacements of the L-rod entrapped in the solid are recorded by two sensors.

B. *Experimental Results*

The recorded temperatures and the horizontal displacement of the solidifying shell, measured with the device of Figure 1 under the previously mentioned conditions, are shown in Figure 2. The data are presented as a function of the distance to the top liquid surface, as measured by the vertical-displacement sensor of the L-rod. The five cooling curves correspond to temperatures measured at the surface of the ingot and at 5, 10, 15, and 20 mm from the surface.

As can be seen from the measured horizontal displacement of the L-rod (ingot contraction curve), there is good contact between the metal and the mold up to about 40 mm below the top surface. The metal then pulls away from the mold at a nearly constant rate. After 250 mm, the L-rod exits the guiding cylinder and the measurement of the ingot contraction terminates.

The five thermocouples indicate a temperature of about 660 °C when the L-rod is inserted in the melt. A fairly good cooling is first induced by direct contact with the mold (primary cooling) before a slight reheating, due to thermal contraction and the formation of an air gap, is observed on the three cooling curves measured closest to the surface. The reheating occurs about 20 mm below the top surface, in apparent contradiction to the length of 40 mm measured for the start of the ingot contraction. As will be shown in Section V, the heat transfer decreases substantially after about 20 mm. This means that the delay between the measured reheating and the ingot contraction is probably due to the inability of the rod to measure very small displacements when the solid shell is not thick enough. At the beginning of pull-in (40 mm), the surface temperature is about 600 °C, which, for the AA5182 alloy, corresponds to a volume fraction of solid of about 70 pct, according to Reference 19. In other words, the contraction of the solidifying shell in the mold already begins when the alloy is in the semisolid state.

The strongest cooling of the ingot is clearly induced by the water jet, whose impingement point is located 70 mm below the top liquid surface (arrow in Figure 2). Due to the high thermal conductivity of aluminum, the five measured temperatures start to decrease rapidly before this point. This is known as the "advanced cooling" effect.[8–13] The corresponding surface temperature of the ingot just below the impingement of the cooling-water jet is about 150 °C.

Below the impingement point, the temperature measured at the surface of the ingot rapidly decreases to almost 50 °C. Since the thermocouple legs emerge at the ingot surface (Figure 1), this measurement can be influenced by the cooling water itself: this explains the oscillations observed on this curve below the water-impingement point. As a consequence, these surface temperatures are only used before the impingement point in the inverse analysis presented in Section V. This corresponds to temperatures higher than 200 °C. Nevertheless, the measured increase in temperature below this point can be related to the observed bounce-off of the water from the ingot surface during the experiment (reduction in the heat transfer), which occurs with a high velocity and/or high impingement angle of the water jet.[9,10]

Assuming that the cooling profiles (deduced from the cooling curves) are representative of the permanent thermal state of the ingot, then the thermal conductivity of the alloy and the distribution of the heat flux along the ingot surface can be deduced by the inverse method presented in the following section.

III. INVERSE METHOD

Inverse methods can be used in solidification and related processes for estimating the boundary conditions and/or physical properties of materials. These methods are based upon a minimization of the errors between calculated and measured temperatures at given locations and times, the calculated values being obtained from a numerical solution of the heat-flow equation. In the present case, the MAP technique, which was developed originally by Milano and Scarpa,[17] is used. Implemented in a finite-element code by Rappaz *et al.*[1] for transient thermal problems, it is extended here to the treatment of permanent temperature situations.

Let us consider a domain (Ω) corresponding to the solidifying ingot or to part of it, within which the steady-state heat-flow equation, including phase transformation and transport of the solid, has to be solved. In the domain, the temperatures (T_j^m) have been measured at a number (N_m) of locations (x_j, where $j = 1, N_m$): they are fixed and known. Using these values, a set of unknown parameters (N_b, where $\mathbf{b} = (b_1, b_2, \ldots, b_{nb})$) is determined *via* the minimization of the function[1]

$$S(\mathbf{b}) = \sum_{j=1}^{N_m} \frac{1}{\sigma_T^2} (T_j^m - T_j^c(\mathbf{b}))^2 + \sum_{k=1}^{N_b} \frac{1}{\sigma^2{}_k} (b_k - b_k^0)^2 \qquad [1]$$

where $T_j^c(\mathbf{b})$ are the calculated temperatures at the positions

x_j, with the (yet unknown) parameters **b**. The standard deviation (σ_T) is a typical error associated with the temperature measurement, whereas the corresponding deviation (σ_k) is a typical interval within which each of the parameters b_k is allowed to vary around an *a priori* (*i.e.*, guessed) parameter (b_k^0). The MAP algorithm returns to the standard least-squares method when the σ_k values are all set to infinity. On the other hand, the parameter b_k will be fixed to the guessed value if the corresponding deviation is made very small.

The parameters to be adjusted, **b**, can be among the following.

(1) Tabulated thermophysical properties, *e.g.*, $\mathbf{b} = (\kappa_1, \kappa_2, \ldots, \kappa_{N_b})$, where the κ_k values are the values of the thermal conductivity of the medium at some tabulated temperature, (T_k). The values of κ in each interval (T_k, T_{k+1}), are linearly interpolated.
(2) Coefficients of a temperature-dependent thermophysical property function, *e.g.*, $\kappa = \beta_1 + \beta_2 T + \beta_3 T^2 + \ldots + \beta_{N_b} T^{N_b-1}$.
(3) Temperature-dependent boundary conditions at a given boundary, *e.g.*, $\mathbf{b} = (h_1, h_2, \ldots, h_{N_b})$, where the h_k values are heat-transfer coefficients for a set of given temperatures.
(4) Position-dependent boundary conditions at a given boundary, *e.g.*, $\mathbf{b} = (q_1, q_2, \ldots, q_{N_b})$, where the q_k values are the values of the heat flow leaving a given boundary at tabulated positions (x_k).

In order to minimize $S(\mathbf{b})$, one writes

$$\frac{\partial S}{\partial b_r} = \sum_{j=1}^{N_m} \frac{-2}{\sigma_T^2} (T_j^m - T_j^c(\mathbf{b})) \cdot X_{jr} + \frac{2}{\sigma_r^2} (b_r - b_r^0) = 0 \qquad [2]$$

where X_{jr} is the sensitivity coefficient:

$$X_{jr} = \frac{\partial T_j^c(\mathbf{b})}{\partial b_r} \cong \frac{T_j^c(b_1, \ldots, b_r + \delta b_r, \ldots, b_{N_b}) - T_j^c(b_1, \ldots, b_r, \ldots, b_{N_b})}{\delta b_r} \qquad [3]$$

The term δb_r is an *a priori* variation of the parameter b_r, which is used to calculate the sensitivity coefficients. An iterative procedure is used to find the solution **b** minimizing $S(\mathbf{b})$. In this iterative procedure, the calculated temperatures ($T_j^c(b^{\nu+1})$) at the next iteration ($\nu + 1$) are also linearized:

$$T_j^c(b^{\nu+1}) \cong T_j^c(b^{\nu}) + \sum_{s=1}^{N_b} X_{js} \cdot \Delta b_s \qquad [4]$$

The increments ($\Delta\mathbf{b}$) of the parameters are then found at each iteration as the solution of the set of linear equations

$$(A) \cdot \Delta\mathbf{b} = \mathbf{f} \text{ or } \sum_{s=1}^{N_b} A_{rs} \cdot \Delta b_s = f_r \qquad [5a]$$

with

$$A_{rs} = \sum_{j=1}^{N_m} \frac{X_{js} X_{jr}}{\sigma_T^2} + \frac{\delta_{rs}}{\sigma_r^2} \qquad [5b]$$

$$f_r = \sum_{j=1}^{N_m} \frac{1}{\sigma_T^2} (T_j^m - T_j^c(\mathbf{b}^{\nu})) X_{jr} - \frac{1}{\sigma_r^2} (b_r^{\nu} - b_r^0) \qquad [5c]$$

where δ_{rs} is the Kroneker symbol.

The MAP inverse method (Eqs. [5a] through [5c]) can be implemented in a fairly simple way in a direct program that can calculate $T_j^c(\mathbf{b})$ when the parameters are known. The iterative procedure is as follows.

(1) At the beginning of the iterations ($\nu = 0$), the components of vector **b** are initiated to some values ($\mathbf{b}^{(\nu=0)}$).
(2) The temperatures ($T_j^c(\mathbf{b}^{\nu})$) are calculated with the direct code.
(3) Each of the parameters b_r is varied by δb_r and the temperatures are again calculated. Using Eq. [3], the sensitivity coefficients (Eq. [3]) are deduced.
(4) Using Eqs. [5a] through [5c], the Nb × Nb system of equations is solved to deduce the increments. If the maximum relative variation of the parameters (Max $|\Delta b_k/b_k|$) is smaller than a desired tolerance, the calculation is finished. If not, the b_k values are updated (*i.e.*, $b_k^{(\nu+1)} = b_k^{\nu} + \Delta b_k$), and the calculation proceeds with the next iteration (step 2) ($(\nu + 1) \rightarrow \nu$).

Please note that, within each iteration, ($N_b + 1$) direct problems are solved with the direct code (the aforementioned steps 2 and 3). This can be fairly central processing unit–intensive, especially if the problem is three-dimensional, the number of parameters is large, and the convergence is slow (*e.g.*, strong nonlinear dependence of the solution with respect to some of the parameters to be fitted). In two dimensions, this problem is less critical.

The success of the inverse method can be measured by the "closeness" obtained between the experimental and simulated values. It can be measured by the residual,

$$R(\mathbf{b}) = \sqrt{\frac{1}{N_m} \sum_{j=1}^{N_m} (T_j^m - T_j^c(\mathbf{b}))^2} \qquad [6]$$

In the present case, the MAP algorithm has been implemented for steady-state problems as a main program, calling the two-dimensional direct FEM heat-flow code CalcoMOS[17] as a subroutine. Using an enthalpy method to treat the latent heat release during solidification, this software can solve, in particular, the heat-flow equation with an advection term,

$$\frac{DH}{Dt} = \frac{\partial H}{\partial t} + \mathbf{V} \cdot \mathbf{grad}\ \mathbf{H} = \text{Div}\ (\kappa(T)\ \mathbf{grad}\ \mathbf{T}) \qquad [7]$$

where $\kappa(T)$ is the temperature-dependent thermal conductivity of the alloy, H is the enthalpy per unit volume, and **V** is the casting speed. The term $\mathbf{V} \cdot \mathbf{grad}\ \mathbf{H}$ accounts for the vertical flow of matter through the computation domain (Eulerian description). Although CalcoMOS can calculate fluid flow in the liquid sump, the associated convective heat transport has not been considered in the present analysis. Please note that, although steady-state is considered here, the term $\partial H/\partial t$ has been kept in this nonlinear problem as an iteration method to reach this state. In order to reduce the calculation time, the computation is started from an initial temperature distribution already very close to the resulting steady-state conditions.

In the two following sections, the inverse method is applied to the permanent situation of the DC casting process, in order to determine the temperature-dependent thermal conductivity of the alloy and the boundary conditions.

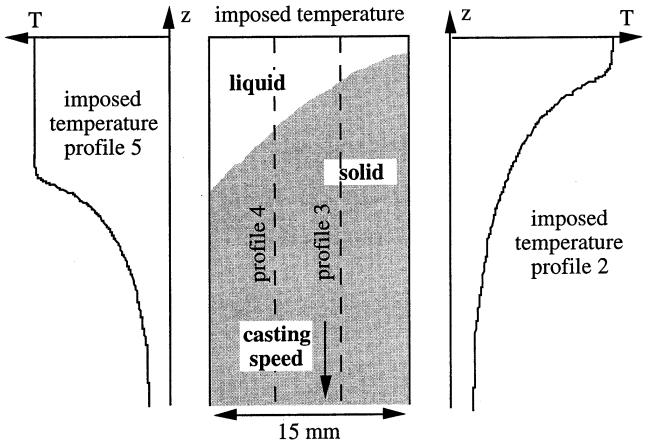

Fig. 3—Computation domain and boundary conditions used for the determination of the thermal conductivity of the alloy.

IV. DETERMINATION OF THE THERMAL CONDUCTIVITY

In contrast to the specific heat, the thermal conductivity of aluminum alloys is highly dependent on the alloying elements or impurities, even at low concentrations. Using the inverse method described in the previous section and the experimental data given in Section II, the temperature-dependent thermal conductivity of the AA5182 alloy is determined in the range of interest, *i.e.*, between 670 °C and about 100 °C. Owing to some uncertainty in the signal provided by the thermocouple located at the ingot surface, this measurement is discarded, and only four measured temperature profiles provided by the L-rod experiment are used in the present calculation.

The computation domain is schematically represented in Figure 3. It corresponds to a vertical rectangular section of the solidifying metal bounded by the top liquid surface, a depth of 300 mm below this top surface, and two vertical lines corresponding to the position of the second and fifth thermocouples (*i.e.*, 5 and 20 mm from the vertical ingot surface). Dirichlet boundary conditions (given temperatures) are applied on the four faces of the domain. On the two vertical boundaries, the temperature profiles measured by the two thermocouples are imposed. At the upper and lower boundaries, an interpolation of the temperatures measured by the four thermocouples is applied. The temperature profiles measured by thermocouples 3 and 4 (10 and 15 mm inside the casting) are then used in the inverse steady-state method to deduce the thermal conductivity of the alloy at six tabulated temperatures ($N_b = 6$). The initial values are set to 150 W/m K at each temperature, and the σ_k values are all put also to 150 W/m K. The standard deviation was set to 1 °C. It should be pointed out that CalcoMOS uses linear interpolations between these tabulated values.

The final result of the inverse method after convergence (black squares) is shown in Figure 4. The thermal conductivity slightly increases with temperature in the solid state and drops to about 100 W m^{-1} K^{-1} in the liquid state. For comparison, the data from other investigations are also plotted in this graph. As can be seen, the present results are in good agreement with the values obtained with the Alstruc software program,[19] but differ substantially from those of

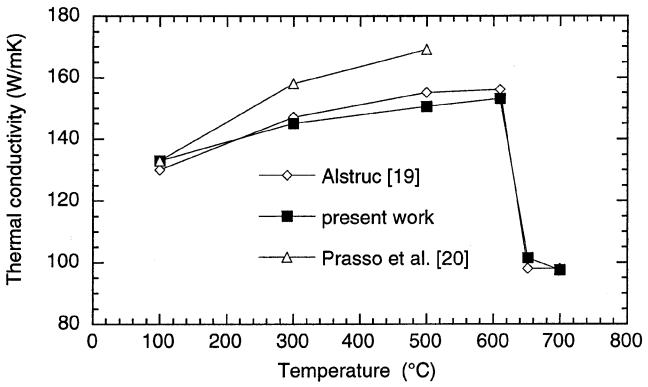

Fig. 4—Computed thermal conductivity of the AA1582 alloy.

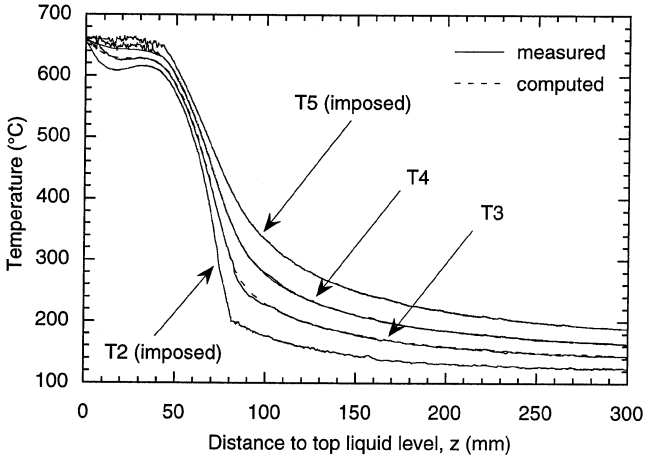

Fig. 5—Computed and measured temperature profiles.

Prasso *et al.*[20] The very good agreement between the computed and measured temperature profiles is demonstrated in Figure 5 and supported by the low final residual (2.5 °C with $N_m = 2400$, Eq. [6]).

The sensitivity of the present analysis to the thermal conductivity was checked by increasing the thermal conductivity found in Figure 4 by 10 pct. In that case, the two computed interior profiles (thermocouples 3 and 4) differed substantially from the measured ones, and the error increased from 2.5 °C to 3.6 °C.

V. DETERMINATION OF THE LATERAL BOUNDARY CONDITIONS

Using the temperature-dependent thermal conductivity obtained in Section IV, the vertical heat-flux distribution along the rolling faces of the ingot is now determined. The method is the same, but the computation domain shown in Figure 6 extends from the lateral surface up to the position of thermocouple 5 (20 mm inside). Keeping the same Dirichlet boundary conditions for the top, bottom, and left-side boundaries of the domain (*i.e.*, in this last case, given by the temperature profile 5), the boundary condition on the right-hand-side boundary can now be determined, based on the four temperature profiles measured at 0, 5, 10, and 15 mm and on the ingot surface temperatures measured above the impingement point, as stated in Section II. It is searched in

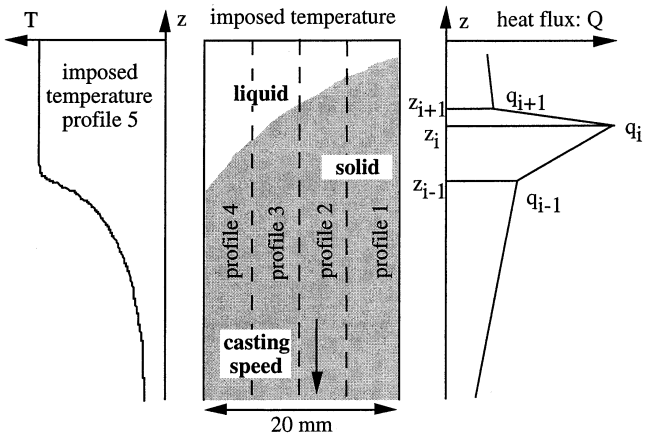

Fig. 6—Computation domain and boundary conditions used for the determination of the cooling condition.

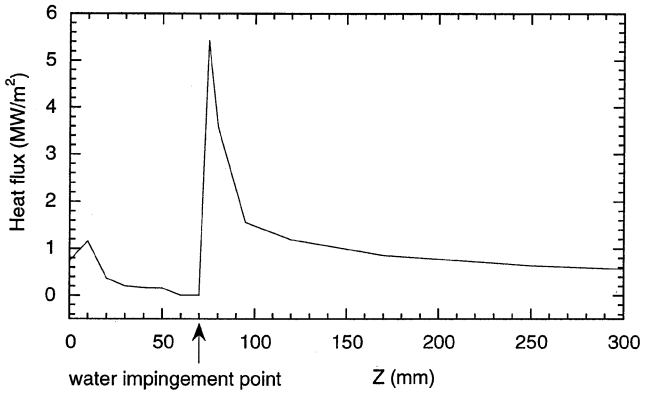

Fig. 7—Computed heat flux as a function of the distance to the top liquid level.

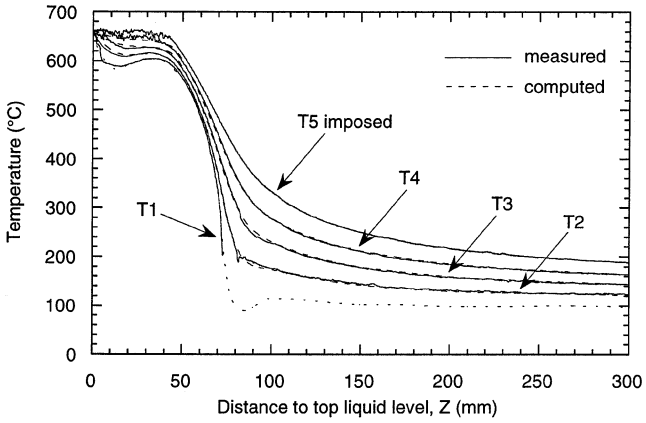

Fig. 8—Computed and measured temperature profiles.

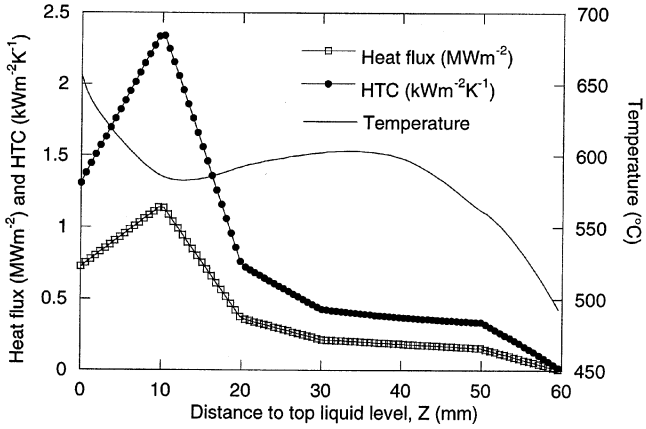

Fig. 9—Computed heat flux, heat transfer coefficient, and surface temperature in the primary cooling zone.

the form of 15 values of the heat flow (q_j), defined at 15 heights along this boundary. These positions are fixed in relation to the contact zone and the position of the impingement point of the water jet. The initial values of the sought heat fluxes, as well as the σ_k values, are set to 0.2 M W m^{-2} in the contact zone and to 2 M W m^{-2} below the water-impingement point.

It should be pointed out that the determination of the horizontal heat-flux distribution along the vertical boundary is much more reliable than the search for a boiling curve (*i.e.,* the temperature-dependent heat-transfer coefficient), since, in this last case, the unknown heat flux depends also on the solution *via* the computed surface temperature.[2] Please note again that CalcoMOS uses linear interpolations between the tabulated heat-flow values.

The distribution of the calculated heat flux along the vertical face of the ingot is shown in Figure 7. The primary cooling zone, the air-gap region, and the effect of the secondary cooling are clearly visible in this figure. As soon as the metal comes in contact with the mold, it is cooled with a heat flux of about 1 M W m^{-2}. The heat flux then decreases to almost zero, due to the formation of the air gap between the metal and the mold. At the impingement point of the water jet, the heat flux increases rapidly to a maximum of about 5.5 M W m^{-2}. It then decreases slowly with increasing distance from the impingement point. The maximum heat-flux, the so-called "critical" heat flux, is reached during boiling, just before the onset of the transition and the film boiling.[8,9,10] The temperature profiles calculated with these boundary conditions are compared to the measurements in Figure 8. Again, good agreement is achieved, and the final residual is only 3.06 °C (N_m = 3880).

Knowing the heat flux, the temperature-dependent heat-transfer coefficient in the primary cooling zone can be determined, assuming a constant mold surface temperature of 100 °C. The result is shown in Figure 9, together with the computed surface temperature of the ingot and the corresponding heat-flux distribution. The maximum heat-transfer coefficient just before reheating and air-gap formation is found to be slightly larger than 2 kW m^{-2} K^{-1}, a value in good agreement with the result of Bakken and co-workers.[11,12] This value decreases rapidly over a distance of 10 to 20 mm as the air gap forms. In spite of the vanishing heat flux, the surface temperature decreases again after 40 mm as a result of the "advance cooling effect" already mentioned by several authors.[8–13]

In the secondary cooling zone, the heat-transfer coefficient is also determined, assuming a constant water temperature of 25 °C. The calculated heat flux and heat-transfer coefficient are plotted in Figure 10 as a function of the computed ingot surface temperature. The general form of this boiling curve is similar to those analyzed in detail by Yu[6] and Weckman and Niessen.[8] Starting on the high-temperature

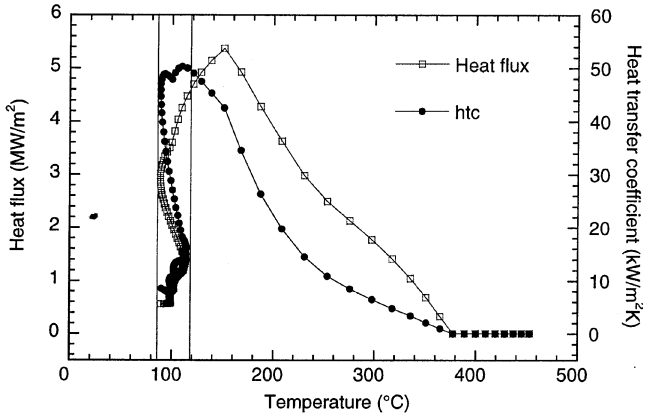

Fig. 10—Computed heat flux and heat transfer coefficient in the secondary cooling zone as a function of the computed surface temperature.

side, the heat flux starts to increase as the temperature decreases below 400 °C. This is the so-called "preimpingement zone."[14] Nevertheless, one should keep in mind that this part of the boiling curve is very sensitive to the positions at which heat fluxes are sought and to the associated linearization used in the inverse method. Unfortunately, with a finer resolution in the determination of the heat-flux distribution, the method becomes unstable because of the lack of a reliable measured surface temperature and of a too-low sampling rate during the measurements.[14]

The heat flux exhibits a maximum of 5.5 M W m^{-2} at a temperature of about 150 °: this corresponds to the position of the water impingement. On the other hand, the maximum in the heat-transfer coefficient is shifted toward a lower temperature (110 °C). The reheating of the ingot surface below the water-impingement point associated with the water bounce-off (Figure 2) produces a somewhat "skewed" cooling curve around 100 °C. In other words, the relationship between the surface temperature and the heat-transfer coefficient is not unique between 90 °C and 110 °C (note the region outlined by two vertical lines in Figure 10). This might be due to the fairly crude assumption of a constant water temperature. More-sophisticated models, in which the increase in water temperature is calculated and different zones near the impingement point are distinguished, should be used instead.[13,14] However, the exact altitudes of the different boundaries of the three zones are not known either, thus adding three unknowns to the problem.

Nevertheless, the shape and the maximum heat flux found here are in good agreement with the findings of Opstelten and Rabenberg[14] for the same alloy. Bakken and co-workers[11,12] also reported very similar results.

VI. CONCLUSIONS

A simple and reliable technique for the measurement of cooling conditions and lateral contraction in DC casting of aluminum alloys has been presented. Based on the design of Drezet *et al.*,[3] it involves an elbowed stainless steel tube (L-rod), in which five thermocouples were introduced, immersed from the top in the melt pool.

Assuming steady-state conditions, the measured cooling curves were converted into temperature profiles. These experimental data were then used in an inverse method to determine the thermal conductivity of the alloy during solidification as a first step, and the distribution of the heat flux on the surface of the ingot as a second step. This inverse method, based on the MAP algorithm,[1] has been adapted to the steady-state temperature field and implemented in the CalcoMOS software program.

The combination of the L-rod technique with the inverse method represents an efficient and robust way to study the conditions in which metal solidifies during DC casting. Besides thermophysical properties, the primary and secondary cooling characteristics can be determined, and the findings are in good agreement with previous results published in literature. The influence of various parameters (*e.g.*, the addition of CO_2, or pulsed water) could be studied in this way. The accuracy of the cooling parameters, especially in the transition region between primary and secondary cooling, is of importance for a better understanding and modeling of the surface segregation and exudations. It is also essential for the prediction of deformations and stresses in the ingot and of the possible formation of hot tears of the shell.

ACKNOWLEDGMENTS

This research was carried out as part of the Brite-Euram project BE-1112 EMPACT (Contract No. BRPR-CT95-0112). It includes the partners Alusuisse-Lonza Services Ltd., Chippis, (Switzerland), Calcom SA (Lausanne, Switzerland), Delft University of Technology (Netherlands), École Polytechnique Fédérale de Lausanne (Lausanne, Switzerland), Elkem Aluminum ANS (Kristiansand, Norway), Hoogovens R&D (IJmuiden, Netherlands), Hydro Aluminum AS (Norway), Institute National Polytechnique de Lorraine, Nancy, France (Péchiney CRV, Voreppe, France), VAW aluminum AG (Bonn, Germany), and SINTEF (Oslo, Norway), as a major subcontractor. The authors thank Dr. B. Magnin (Péchiney), Dr. I. Opstelten and J. Rabenberg (Hoogovens), Ivar Farup (SINTEF), and E.-K. Jensen (Elkem) for their valuable comments to this work. Funding by the European Community and by the Office Fédéral de l'Education et de la Science (Berne) for the Swiss partners is gratefully acknowledged.

REFERENCES

1. M. Rappaz, J.-L. Desbiolles, J.-M. Drezet, C.-A. Gandin, A. Jacot, and P. Thévoz: in *Modeling of Casting, Welding and Advanced Solidification Processes*, M. Cross and J. Campbell, eds., TMS, Warrendale, PA, 1995, pp. 449-57.
2. J.-M. Drezet: Ph.D. Thesis No. 1509, EPF-Lausanne, Lausanne, 1996.
3. J.-M. Drezet, M. Rappaz, B. Carrupt, and M. Plata: *Metall. Mater. Trans. B*, 1995, vol. 26B, pp. 821-30.
4. A. Mo, T. Rusten, H.J. Thevik, B.R. Henriksen, and E.K. Jensen: in *Light Metals 1997*, R. Huglen, eds., TMS, Warrendale, PA, 1997, pp. 667-74.
5. J.-M. Drezet and M. Rappaz: *Metall. Mater. Trans. A*, 1996, vol. 27A, pp. 3214-25.
6. H. Yu: *Light Metals 1980*, TMS, Warrendale, PA, 1980, pp. 613-28.
7. F.P. Incropera and D.P. de Witt: *Fundamentals of Heat and Mass Transfer*, John Wiley & Sons, New York, NY, 1985, p. 461.
8. D.C. Weckman and P. Niessen: *Metall. Trans. B*, 1982, vol. 13B, pp. 593-602.
9. J.F. Grandfield, A. Hoadley, and S. Instone: in *Light Metals 1997*, R. Huglen, ed., TMS, Warrendale, PA, 1997, pp. 691-99.
10. J.F. Grandfield, K. Goodall, P. Misic, and X. Zhang: in *Light Metals*

1997, R. Huglen, ed., TMS, Warrendale, PA, 1997, pp. 1081-90.
11. J.A. Bakken and T. Bergstrøm: *Light Metals 1986*, TMS, Warrendale, PA, 1986, pp. 883-89.
12. E.K. Jensen, S. Johansen, T. Bergstrøm, and J.A. Bakken: *Light Metals 1986*, TMS, Warrendale, PA, 1986, pp. 891-96.
13. L. Maenner, B. Magnin, and Y. Caratini: in *Light Metals 1997*, R. Huglen, ed., TMS, Warrendale, PA, 1997, pp. 701-07.
14. I. Opstelten and J. Rabenberg: in *Light Metals 1999*, C. Eckert, ed., TMS, Warrendale, PA, 1999, pp. 729-35.
15. J.V. Beck, B. Blackwell, and C.R. St Clair, Jr.: *Inverse Heat Conduction—Ill-Posed Problems*, Wiley, New York, NY, 1985.
16. J.V. Beck and K.J. Arnold: *Parameter Estimation in Engineering and Science*, Wiley, New York, NY, 1977.
17. G. Milano and F. Scarpa: Universita di Genova, Italia, private communication, 1994.
18. P. Thévoz, M. Rappaz, and J.L. Desbiolles: in *Light Metals 1990*, C.M. Bickert, ed., TMS, Warrendale, PA, 1990, pp. 975-84.
19. A.L. Dons, E.K. Jensen, Y. Langsrud, E. Trømborg, and S. Brusethaug: in *Metall. Mater. Trans. A*, 1999, vol. 30A, pp. 2135-46.
20. D.C. Prasso, J.W. Evans, and I.J. Wilson: *Metall. Mater. Trans. B*, 1995, vol. 26B, pp. 1281-87.
21. J.A. Dantzig: *Rev. Sci. Instrum.*, 1985, vol. 56 (5), pp. 723-25.